Notes about the limits of ultra-high speed solid-state imagers

R. Turchetta

Rutherford Appleton Laboratory, Science and Technology Facilities Council (STFC), Harwell Science and Innovation Campus, Didcot, OX11 0QX, U.K, e-mail: renato.turchetta@stfc.ac.uk

Introduction

In recent years, there has been an increase in the offering for solid-state sensors for ultra-high speed imaging, i.e. for frame rates in excess of 1 million per second. CCD In-Situ Image Sensors (ISIS) were proposed in 1999 [1, 2] and recently CMOS options have become available, with CCD storage in CMOS [3, 4], CMOS full frame transfer [3] and pixel multiplexing [6]; SPADs sensors have also been mentioned in the context of ultra-high speed imaging [7]. With frame rates above 10^6 and moving towards 10^9 per second, it feels timely to make some considerations on the limits of ultra-high speed solid-state imagers, namely those due to the movement of the photon-generated charge and, for photon counting sensors, to dead time.

The Shockley-Ramo's theorem.

With frame rates moving towards 10^9 per second, even at the saturated velocity, a charge carrier would move by 100 µm in one ns in silicon. In other words, we are approaching a similar situation found in the 30's by those people working with vacuum tubes when 'the time of transit of the electron is of comparable duration with the periods of alternating circuits' [8]. By choosing an appropriate weighting field $\overrightarrow{E_W}$ and then using Green's theorem [9], Shockley [8] and, one year later and independently, Ramo [10] demonstrated that, given an arbitrary configuration of electrodes C_1, … C_4 held at a fixed potential V_1 … V_4 respectively (Figure 1), the instantaneous current $i_k(t)$ seen by k-th electrode and due to the movement of charge q with velocity $\vec{v}$ is given by:

$$i_k(t) = q\,\vec{v}\cdot\overrightarrow{E_W} \qquad (1)$$

The velocity $\vec{v}$ varies with time due to the movement of the charge and is given by $\vec{v} = \mu\vec{E}$, where µ is the mobility and $\vec{E}$ is the electric field at the point where the charge is. The weighting field $\overrightarrow{E_W}$ is calculated by grounding all electrodes and setting a unity potential on the k-th electrode, i.e. the electrode for which we want to calculate the current. For semiconductors, where fixed charge is present in the sensing volume, it can be shown that the weighting field has to be calculated in the absence of any space charge. So for a simple 1-d p-n junction with a width w, the weighting electric field is simply given by 1/w. The unit of the weighting field is simply the inverse of a distance, or, in other words, the weighting potential had no dimensions.

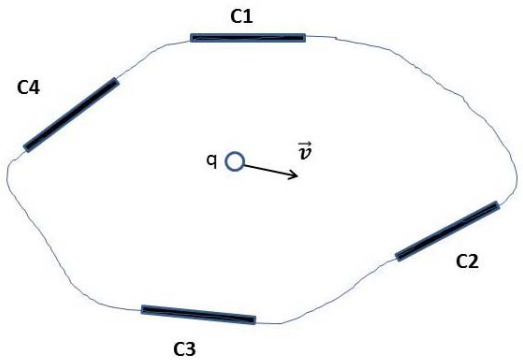

Figure 1. Geometrical configuration used in the Shockley-Ramo's theorem.

The highlight of equation (1) is that the instantaneous current is due to the movement of charges not their collection. The integral over time of this current will correctly give the amount of collected charge, so if the transit time of a carrier is negligible with respect to the frame time, the conventional belief that the signal is determined by the collected charge, still holds. It should also be noted that in the case of semiconductors, both generated carriers, i.e. electrons and holes, will independently generate a current. The total measured current, given by the sum of the two carriers' contributions, is the one whose integral is equal to the collected charge. However, if taken separately, one type of carriers would only give a fraction of the total charge, whose amount would depend on the position where the carrier was generated in the semiconductor. It should also be noticed that in (1), the operation is a scalar product so if a carrier moves in a direction perpendicular to the weighting field, no current will be induced.

Monte Carlo simulation

In order to explore the limit on frame rate due to (1), a 1-d Monte Carlo simulation was built. The geometry of the simulation is shown in fig. 2. It corresponds to a one-sided abrupt junction, with the N-side much more heavily doped than the P-side so that the depletion region can be considered to extend only in the P-substrate. Depending on the doping, total thickness wtot and bias of the junction, the P-type region can be partially depleted, as shown in the figure, or totally depleted. If the applied bias exceeds the minimum needed to fully deplete the P-region, over-depletion will occur, i.e. the minimum electric field in the depleted region will be non-null [12]. In the simulation, the movement of carriers is also affected by diffusion, which has a zero net effect with a standard deviation given by $\sqrt{2Dt_{tr}}$, where D=kTμ/q is the diffusion constant and t_{tr} is the transit time of the carrier. Velocity saturation effects were taken into account by modelling the speed according to the equation

$$v = \frac{\mu_0 E}{\left[1+\left(\frac{\mu_0 E}{v_s}\right)^{\alpha}\right]^{1/\alpha}} \qquad (2)$$

where μ_0 is the low-field mobility, v_s is the saturation velocity and α is a constant which is equal to about 2 for electrons and about 1 for holes [13].

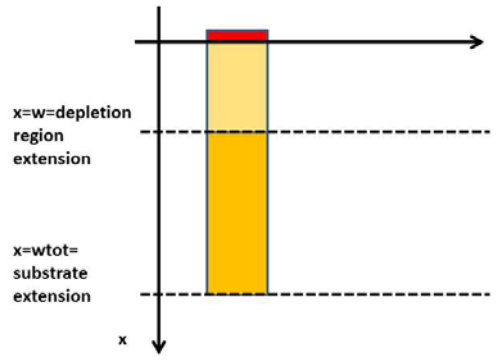

Figure 2. Geometry used in the MC simulation.

A specific wavelength was selected for each simulation run and 2,000 electron-hole carriers were generated at a random depth following an exponential distribution with parameter set by the absorption length for the given wavelength.

The difference between the current signal as calculated by (1) and the one related to the collection of the carrier collected at the electrode where the current is measured is well illustrated by Figure 3. In this case, the total epi thickness was 5 um and the applied bias 1.5V for a low resistivity substrate, doped at $2*10^{15}$ cm^{-3}. The sensor is front-illuminated, i.e. the light is coming into from the N-side and the wavelength is 450nm. The integral of (1) is plotted in the figure, with a fixed right limit at t=0, i.e. when the charge is created. The electrons (dashed line) are collected very quickly, mostly within the first ns, but their contribution to the total current is very small as they do not travel for any significant length. Holes (dotted) are much slower and contribute to most of the signal (solid). It should be noted that the diffusion current from the substrate is not considered in this simulation, where the substrate is considered as a perfect conductor.

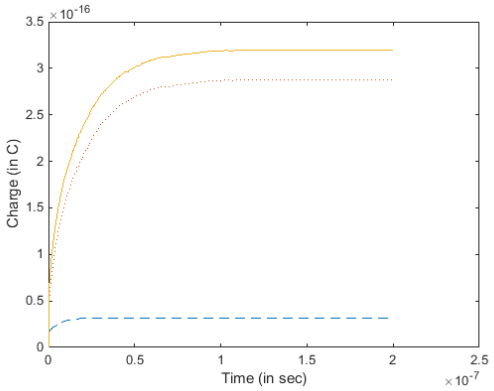

Figure 3. Integrated current for a low resistivity substrate, 5um thick, biased at 1.5V. Electrons' (dashed), holes' (dotted) and total integrated charge are plotted.

The Shockley-Ramo's theorem was used to evaluate differences in measured current due to signals generated by different colours. This is shown in Figure 4 for different wavelengths, all other parameters being the same as in Figure 3. The four curves reach 90% of the total integrated charge after 24.2 32.4, 38.8 and 39.1 respectively for decreasing wavelength. When sampling the signal at high speed, colour mixing in different temporal frames would then happen. Figure 5 illustrates what happens in the case of back-side illumination. In this case, the fastest signal is the blue signal as this is dominated by the movement of the electrons, while the IR signal has a fast component due to the movement of electrons, but then a much slower rise due to the hole, generated deep in silicon and travelling all the way from the front to the back surface.

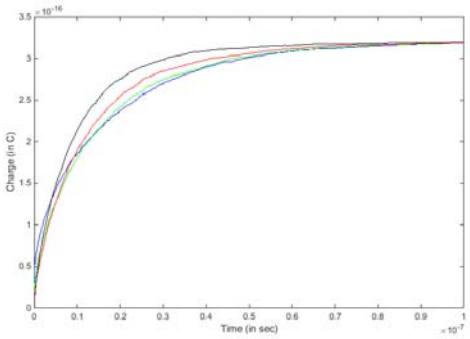

Figure 4. Total integrated currents measured for different colours: 450 nm (blue), 550 nm (green), 650 nm (red) and 800 nm (black). All other parameters as in fig. 3.

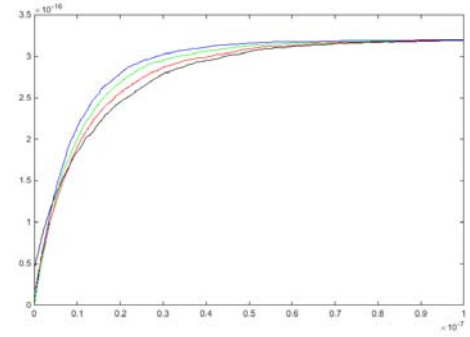

Figure 5. As above, but for back-side illumination (BSI).

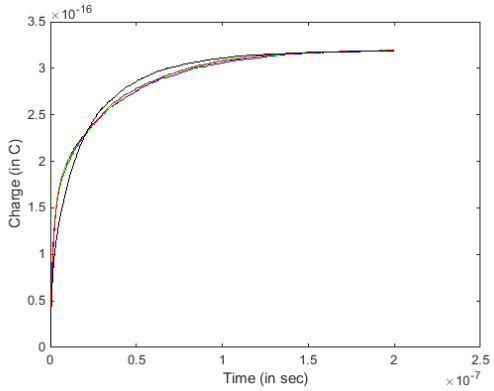

Figure 6. As above, but for a high-resistivity, 12 µm thick epi, in front-illumination (FSI).

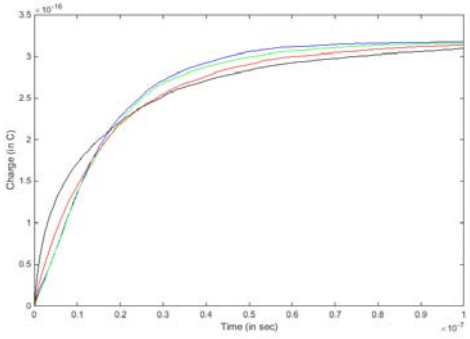

Figure 7. As for fig. 6, but in BSI.

Fig. 6 and 7 give the same curves for a high-resistivity ($2*10^{13}$ cm^{-3} doping), 12 µm thick epi, for the case of front- and back-side illumination respectively. The applied bias is still 1.5V, which is not enough to fully deplete the epi. It is interesting to notice that colour separation is much less severe for the FSI case then for BSI. However the charge collection is much faster in this latter case, so that spatial cross-talk would be much reduced.

Applying a higher bias to fully deplete the entire volume of the epitaxial layer greatly improves the situation as shown in Figure 8.

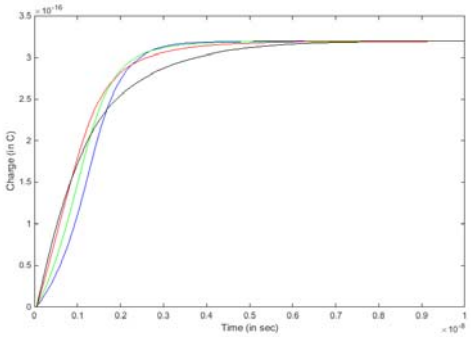

Figure 8. As in figure 7, but for an applied bias of 5 V, which is enough to fully deplete the substrate. Worth noticing that the time axis is zoomed 10 times with respect to all other figures.

Deadtime

In SPAD, the sensitive volume tends to be shallower thus making these sensors very fast and able to achieve timing resolution well below 1 ns. The quenching and re-charge circuitry tend to introduce a dead time. This dead time sets a limit to the number of photons that each pixel can count in a given period, thus introducing a dependence of the maximum frame rate on the resolution of the image for imaging applications.

The exact influence of the dead time t_{dead} over the maximum counting frequency depends on the type of pixel circuitry. Figure 9 shows the relationship between the photon arrival frequency (assuming 100% QE, for sake of simplicity) and the measured counting frequency, and this for two very common models of t_{dead}, called 'paralysable' and 'non-paralysable'. For both configurations, the t_{dead} is set to 1µs. The figure shows that, due to the Poisson statistics of photon arrival time, even in the relative benign case of a non-paralysable system, corrections to photon counting are necessary for photon arrival frequencies well below 1MHz. Shorter t_{dead} and different t_{dead} models would yield different limitations [15],

but this shows that some care has to be taken to be able to use a SPAD up to a counting frequency equal to $1/t_{dead}$.

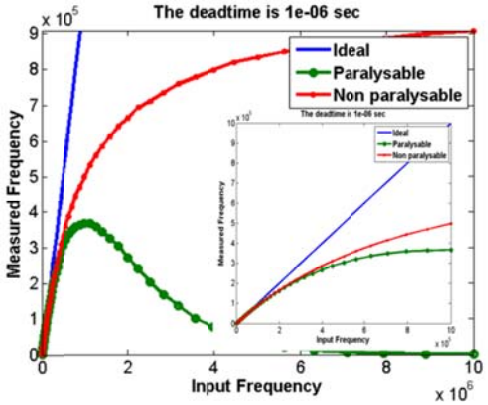

Figure 9. Measured frequency as a function of input frequency for a counting system for different deadtime models and the ideal situation.

Conclusions

The Shockley-Ramo's theorem allows calculation of the current signal in a semiconductor device even for the situation where the charge carrier's transit time is comparable to the speed at which the signal is sampled. This induced current is generated by the movement of charge, so that the current signal is given by the movement of carriers and not by their collection. We analysed the effect of this theorem with the help of a 1-D Monte Carlo simulation. For a given device, more complete TCAD modelling should be performed in order to get more accurate results, however the 1-D simulation allows getting a fast grip over the effect of the theorem and shows that the result can be very different from what conventionally believed. The simulation shows that attention should be paid to the biasing and electrode configurations in order to avoid colour mixings in consecutive frames.

The last section of this paper deals with dead time modelling. SPAD has a very fast response time, well below 1 ns, but their ability to be used in imaging applications by counting photons is limited by the dead time. For a given frame rate, the image accuracy would depend on the dead time of the SPAD, with the exact relationship being determined by the type of deadtime.

References

[1] T. Etoh, H. Mutoh and K. Takehara, *A CCD-CMOS Image Sensor for Ultra-High Speed Image Capturing*, in Proc. IEEE Workshop on CCDs & AIS, Japan, June 1999

[2] T. Arai, et al., *A 252-V/lux•s, 16.7-Million-Frames-per-Second 312-kpixel Back-Side-Illuminated Ultrahigh-Speed Charge-Coupled Device*, IEEE TED, vol. 60, no. 10, pp. 3450-3458, Oct. 2013

[3] J. Crooks et al., *Kirana: a solid-state megapixel uCMOS image sensor for ultra-high speed imaging*, in Proc. of SPIE Conf., Electronic Imaging, vol. 8659, 201

[4] A. Lahav et al., *CMOS Image Sensor Pixel with 2D CCD Memory Bank for Ultra High Speed Imaging with Large Pixel Count*, in Proc. of the 2013 IISW

[5] Y. Tochigi, et al., *A Global-Shutter CMOS Image Sensor with Readout Speed of 1Tpixel/s Burst and 780Mpixel/s Continuous*, ISSCC Dig. Tech. Papers, pp. 382-383, Feb. 2012

[6] F. Mochizuki et al., *Single-Shot 200Mfps 5x3-Aperture Compressive CMOS Imager*, Digest of ISSCC 2015, 116-118

[7] T. Etoh et al., *Toward One Giga Frames per Second - Evolution of in Situ Storage Image Sensors*, Sensors 2013, 13(4), 4640-4658

[8] W. Shockley, *Currents to conductors induced by a moving point charge*, J. Appl. Phys. 9 (1938) 635

[9] J. D. Jackson, *Classical Electrodynamics*, John Wiley and Sons, 1974

[10] S. Ramo, *Currents induced by electron motion*, Proc. of the I.R.E., 1939, 584-585

[11] G. Cavalleri et al., *Extension of Ramo's Theorem as applied to induced charge in semiconductor detectors*, Nucl. Instr. And Methods, 92 (1971) 137—140

[12] E. Gatti – P. F. Manfredi, *Processing the signals from solid-state detectors in elementary-particle physics*, La Rivista del Nuovo Cimento, vol. 9, serie 3, 1986

[13] S. M. Sze and K. K. Ng, *Physics of Semiconductor Devices*, John Wiley and Sons, 2007

[14] Glenn F. Knoll, *Radiation Detection and Measurement*, John Wiley & Sons, 2010

[15] A. Eisele et al., *185 MHz Count Rate, 139 dB Dynamic Range Single-Photon Avalanche Diode with Active Quenching Circuit in 130 nm CMOS Technology*, Proc. of IISW 2011, Japan